Inorganic Chemistry

Article

pubs.acs.org/IC

Photochemistry and Photophysics of a Pd(II) Metalloporphyrin: Re(I) Tricarbonyl Bipyridine Molecular Dyad and its Activity Toward the Photoreduction of CO_2 to CO

Jacob Schneider,[†] Khuong Q. Vuong,[‡] James A. Calladine,[‡] Xue-Zhong Sun,[‡] Adrian C. Whitwood,[†] Michael W. George,*[,‡] and Robin N. Perutz*[,†]

[†]Department of Chemistry, University of York, York, YO10 5DD, United Kingdom

[‡]School of Chemistry, University of Nottingham, University Park, Nottingham, NG7 2RD, United Kingdom

Supporting Information

ABSTRACT: The photochemistry and photophysics of the cationic molecular dyad, 5-{4-[rhenium(I)tricarbonylpicoline-4-methyl-2,2′-bipyridine-4′-carboxyamidyl]phenyl}-10,15,20-triphenylporphyrinatopalladium(II) ([**Re(CO)$_3$(Pic)Bpy-PdTPP**][**PF$_6$**]) have been investigated. The single crystal X-ray structure for the thiocyanate analogue, [**Re(CO)$_3$(NCS)-Bpy-PdTPP**], exhibits torsion angles of 69.1(9)°, 178.1(7)°, and 156.8(9)° between porphyrin plane, porphyrin-linked C_6H_4 group, amide moiety, and Bpy, respectively. Steady-state photoexcitation (λ_{ex} = 520 nm) of [**Re(CO)$_3$(Pic)Bpy-PdTPP**][**PF$_6$**] in dimethylformamide (DMF) results in substitution of Pic by bromide at the Re(I)Bpy core. When [**Re(CO)$_3$(Pic)Bpy-PdTPP**][**PF$_6$**] is employed as a photocatalyst for the reduction of CO_2 to CO in DMF/NEt_3 solution with λ_{ex} > 420 nm, 2 turnovers (TNs) CO are formed after 4 h. If instead, a two-component mixture of PdTPP sensitizer and mononuclear [Re(CO)$_3$(Pic)Bpy][PF$_6$] catalyst is used, 3 TNs CO are formed. In each experiment however, CO only forms after a slight induction period and during the concurrent photoreduction of the sensitizer to a Pd(II) chlorin species. Palladium(II) *meso*-tetraphenylchlorin, the hydrogenated porphyrin analogue of PdTPP, has been synthesized independently and can be substituted for PdTPP in the two-component system with [Re(CO)$_3$(Pic)Bpy][PF$_6$], forming 9 TNs CO. An intramolecular electron transfer process for the dyad is supported by cyclic voltammetry and steady-state emission studies, from which the free energy change was calculated to be ΔG_{ox}* = −0.08 eV. Electron transfer from Pd(II) porphyrin to Re(I) tricarbonyl bipyridine in [**Re(CO)$_3$(Pic)Bpy-PdTPP**][**PF$_6$**] was monitored using time-resolved infrared (TRIR) spectroscopy in the ν(CO) region on several time scales with excitation at 532 nm. Spectra were recorded in CH_2Cl_2 with and without NEt_3. Picosecond TRIR spectroscopy shows rapid growth of bands assigned to the π–π* excited state (2029 cm^{-1}) and to the charge-separated state (2008, 1908 cm^{-1}); these bands decay and the parent recovers with lifetimes of 20–50 ps. Spectra recorded on longer time scales (ns, μs, and seconds) show the growth and decay of further species with ν(CO) bands indicative of electron transfer to Re(Bpy).

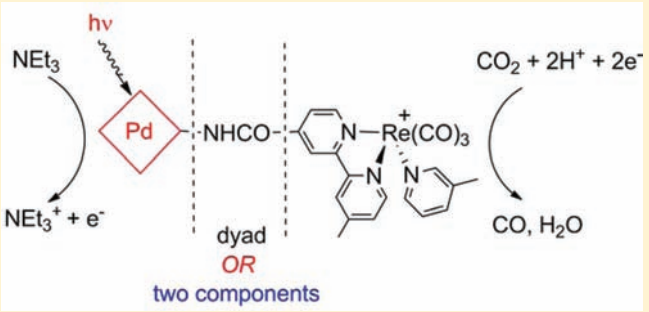

INTRODUCTION

The conversion of light-to-chemical energy is an attractive approach to a sustainable future, and solar fuels provide a means to exploit that energy through concepts of fundamental chemistry.[1] In photosynthesis, plants absorb light energy from the sun to convert CO_2 and water into organic molecules and oxygen, storing energy in the chemical bonds of the newly formed molecules.[2] The *artificial* photocatalytic conversion of CO_2 into liquid fuels with homo- and heterogeneous systems has been a field of interest for many years,[3−5] and though it remains a viable option, great advances are needed to develop a sustainable infrastructure for solar fuels. One possible strategy to utilize CO_2 as a raw material for hydrocarbon products[6,7] is to reduce CO_2 to CO, a chemical feedstock for such industrial processes as hydroformylation[8] and the Fischer–Tropsch reaction.[9] Another strategy for CO_2 reduction is to employ electrocatalytic systems that obtain their electrons from solar cells and are capable of multielectron multiproton processes adept at yielding fuels beyond CO such as MeOH and methane.[10−12]

In the early 1980s, Lehn and Ziessel reported the photochemical reduction of CO_2 to CO using a simple molecular photocatalyst, Re(CO)$_3$(Bpy)X (Bpy = 2, 2′-bipyridine, X = Cl, Br) with blue or near UV light (λ > 400 nm) in DMF/TEOA (DMF = dimethylformamide; TEOA = triethanolamine) solution, with TEOA acting as a sacrificial electron donor.[13,14] They found the homogeneous rhenium(I)

Received: February 21, 2011
Published: November 1, 2011

catalyst to be highly selective for CO production compared to other photocatalytic systems such as $Ru(Bpy)_3^{2+}$,[15] mixtures of $Ru(Bpy)_3^{2+}$ and Co^{2+} (Co^{2+} = $CoCl_2$ or $Co(Bpy)_3^{2+}$),[13,16] or mixtures of $Re(CO)_3(Bpy)X$ and Co^{2+},[13] for which the CO_2 photoreduction products may include formate or H_2. The detailed mechanism of CO_2 reduction using the Re(I) photocatalysts has remained elusive since the seminal work by Lehn and Ziessel and continues to be an area of extraordinary interest.[3,17−19] Their system was recently optimized by Ishitani and co-workers in a mechanistic study that led to the use of two different molecular entities in combination, $Re(CO)_3(Bpy)(MeCN)^+$ serving as a catalyst and $Re(CO)_3((4,4'\text{-}MeO)_2Bpy)(P(OEt)_3)^+$ as the photosensitizer, with a quantum yield of 0.59 for CO formation.[18] One of the drawbacks to using Re(I) tricarbonyl diimine complexes as *photo*catalysts is the high energy light required ($\lambda \sim 350-450$ nm) to induce their metal-to-ligand charge transfer (MLCT) excited-states.[20] Over the past few years Ishitani, Bian, and co-workers attempted to remedy this by sensitizing a molecular Re(I) catalyst with one or more visible-light absorbing $Ru(Bpy)_3^{2+}$ pendants.[21−23] A number of different di- and multinuclear Ru(II)−Re(I) complexes have been synthesized that function as single component photocatalysts in the reduction of CO_2 to CO using lower energy visible light ($\lambda >$ 500 nm).[24,25] The most effective of these are the molecular dyads that have an insulated connection between $Ru(Bpy)_3^{2+}$ and Re(I),[25,26] with $P(OEt)_3$ as the peripheral ligand for $Re(CO)_3(Bpy)$, giving a quantum yield for CO formation of 0.21.[27]

While frequently studied mononuclear Re(I) photocatalysts are of the general formula $[Re(CO)_3(Bpy')(X/L)]^{0/+}$ (X = halide, NCS, CN; L = phosphine, phosphite; Bpy′ = 2, 2′-bipyridine and derivatives),[18,28−30] or even $[Re(CO)_2(Bpy')(L)_2]^+$,[31,32] there is one study that uses mononuclear $[Re(CO)_3(Bpy)(4\text{-}Xpy)]^+$ (Xpy = pyridine derivatives) complexes for the photocatalytic reduction of CO_2.[33] The authors showed that the 4-Xpy family of complexes are not as efficient photocatalysts as their halide and phosphite analogues, having lower quantum yields (ϕ = 0.03−0.13). In addition, Ishitani and colleagues suggested that when pyridine is the peripheral ligand in single component Ru(II)−Re(I) dinuclear complexes, the decomposition of the active photocatalyst is accelerated, thus lowering its catalytic activity.[27] Apart from these reports, the reactivity of mono- and dinuclear complexes with a pyridine bound to Re(I) toward CO_2 reduction remains relatively unexplored. To investigate this further we have built upon our earlier work[34−36] and synthesized a molecular dyad made up of two components: (1) a low-energy-light absorbing Pd(II) metalloporphyrin core that is covalently attached to (2) a photocatalytic Re(I) tricarbonyl bipyridine (Re(I)Bpy) center with 3-picoline as the ancillary ligand.[37] The two components are linked through an amide bond that aims to optimize electron-transfer efficiency. It has been determined in analogous Zn(II) and Mg(II) dyads that there is no communication between metalloporphyrin and Re(I)Bpy in the ground state.[36] However, upon selective light excitation into the metalloporphyrin S_1 state, photoinduced electron transfer occurs,[36] as well as subsequent substitution of 3-picoline by other nucleophiles or solvent molecules at the Re(I)Bpy center.[35−37] In addition, a Zn(II) porphyrin-Re(I)Bpy dyad was recently reported by Inoue and co-workers to undergo electron transfer from the porphyrin S_2 state to the Re(I)Bpy center, a process that also led to the photoreduction of CO_2, with a quantum yield of 0.0064 for CO formation.[38] In a separate study that involved a Zn(II) pyridylporphyrin directly coordinated to a Re(I)Bpy fragment via a pyridine,[39] Alessio, Scandola, and co-workers found the photoinduced charge transfer process from the S_1 state of the Zn(II) porphyrin to Re(I)Bpy to be only slightly exergonic; the complexes were not tried for photochemical CO_2 reduction. Recently, a Zn(II) pyridylporphyrin was linked to a cobaltbis(dimethylglyoximate) moiety and used for the photogeneration of hydrogen in the presence of triethylamine.[40] These reports draw obvious parallels to the current study, but the structural, photochemical, and photophysical properties of the Pd(II) porphyrin−Re(I)Bpy dyad described here are distinct.

In this study the tetraphenylporphyrin sensitizer is coordinated to Pd(II). We investigate the photochemical and photophysical properties of a previously reported single component Pd(II)−Re(I) dinuclear complex, **$[Re(CO)_3(Pic)$-Bpy-PdTPP$][PF_6]$** (Pic = 3-picoline; Bpy = 2, 2′-bipyridine; TPP = *meso*-tetraphenylporphyrin).[37] The complex showed striking activity toward photosubstitution at the Re(I)Bpy center, but the photophysics were not studied in detail. In addition, Pd(II) metalloporphyrins are less familiar in the literature than other metalloporphyrin complexes, especially with regard to supramolecular chemistry. We have examined the time-resolved features of **$[Re(CO)_3(Pic)$Bpy-PdTPP$]$-$[PF_6]$** such as photoinduced charge separation and radical formation that occur from picoseconds up to seconds, as well as its steady-state reactions including remote-site photosubstitution of 3-picoline by bromide and CO_2 reduction to CO. We find that saturation of a C═C bond of the porphyrin to produce a chlorin sensitizer occurs during photocatalysis. We also report systems for the photocatalytic reduction of CO_2 in DMF/NEt_3 solution that involve a two-component mixture of Pd(II) porphyrin or chlorin sensitizer and $[Re(CO)_3(Pic)$-Bpy$][PF_6]$ as a mononuclear catalyst. They yielded slightly higher but still modest amounts of CO.

EXPERIMENTAL SECTION

Characterization and Instrumentation. All NMR spectra were recorded on a Bruker 500 MHz spectrometer. ^1H NMR chemical shifts (in ppm) are referenced using the residual solvent resonances of CD_2Cl_2, $CDCl_3$, or THF-d_8; $^{31}P\{^1H\}$ NMR chemical shifts (in ppm) are relative to an external H_3PO_4 standard. NMR spectroscopic assignments were made with the aid of 2D $^1H-^1H$ COSY analysis. We relied on high resolution mass spectrometry rather than elemental analysis because of incomplete combustion when attempting microanalysis. Solution infrared spectra were measured using a Unicam Research Series FTIR spectrometer in either a demountable Omni cell system (Specac) or a Harrick solution cell with 2 mm CaF_2 windows. Electrospray Ionization (ESI) mass spectra (positive) were recorded on a Bruker microOTOF mass spectrometer coupled to an Agilent 1200 Series LC system. Mass spectra are quoted for $^{106}Pd^{187}Re$. The UV−visible absorption spectra were measured using an Agilent 8453 spectrometer. The emission spectra were measured using a Hitachi F-4500 Fluorimeter, and all samples (1.0×10^{-5} M) were either degassed by three freeze−pump−thaw cycles or deaerated by purging the samples with Ar.

Cyclic voltammograms of **$[Re(CO)_3(Pic)$Bpy-PdTPP$][PF_6]$**, PdTPP, and PdTPC in CH_2Cl_2 were measured using a VoltaLab PST050 potentiostat (Radiometer Analytical) with Pt wire working, Pt wire auxiliary, and Ag wire pseudoreference electrodes. The cyclic voltammogram of $[Re(CO)_3(Pic)Bpy][PF_6]$ in CH_2Cl_2 was measured using a BAS 100B Electrochemical Analyzer with glassy carbon working, Pt wire auxiliary, and SCE reference electrodes. The sample solutions contained 0.1 M $[Bu_4N][PF_6]$ (electrochemical grade,

Aldrich) and were continuously stirred and purged with a steady flow of N_2 or Ar in between measurements. Ferrocene (sublimed, Aldrich) was used as an internal standard during each experiment, and the electrochemical potentials are reported versus the internal ferrocenium/ferrocene ($Fc^{+/0}$) redox couple.

Steady-state photolysis experiments were performed using either a (1) ILC 302UV xenon high intensity light source set to visible (ILC Technology, Inc.) *or* a (2) Hitachi XGA ED-X3270A multimedia mobile data projector (150 W UHB mercury lamp) *or* a (3) BenQ MP77 data projector (Philips 280 W UHB mercury lamp). The light was directed through a water filter (10 cm) and a cutoff or interference filter before reaching the sample solution. Experiments with lamp (2) are summarized in the Supporting Information, Table S1; lamp (3) was only used for the quantum yield measurements outlined below.

The quantum yield (ϕ) for the photosubstitution of 3-picoline by bromide in $[\mathbf{Re(CO)_3(Pic)Bpy\text{-}PdTPP}][\mathbf{PF_6}]$ was calculated using a method developed by Lees,[41] and accounts for the inner filter absorbance of the $[\mathbf{Re(CO)_3BrBpy\text{-}PdTPP}]$ product that is formed (see the Steady-State Photochemistry section of the manuscript for more details). The incident light intensity (BenQ MP777; λ = 520 nm narrow bandwidth filter) reaching the sample during photolysis was 7.5×10^{-9} einsteins s^{-1} (0.51 mW/cm^2), determined using an ILT1400 radiometer (International Light Technologies).

The specifications of pico-, nano-, and microsecond time-resolved infrared spectroscopy experiments have been reported.[42,43] A Nicolet 680 FTIR spectrometer capable of rapid-scanning was synchronized to the laser for the longer time scale measurements. For all TRIR and FTIR experiments the second harmonic output (532 nm) of a Nd:YAG laser was used and the concentrations of $[\mathbf{Re(CO)_3(Pic)\text{-}Bpy\text{-}PdTPP}][\mathbf{PF_6}]$ and NEt_3 (when present) were approximately 0.5 mM and 1 M in CH_2Cl_2, respectively.

Photochemical Reduction of CO_2. All photochemical CO_2 reduction experiments were carried out in a custom-designed photolysis kit fitted with a gas infrared cell (100 mm long, 25 mm diameter CaF_2 windows) connected to a UV−visible cuvette (10 mm path length) (See the Supporting Information, Figure S1). A 3 mL solution of either 0.05 or 0.27 mM complex in DMF/NEt_3 (5:1 v/v) was transferred to the UV−visible cuvette and sealed with a red rubber Suba-seal and wire. The sample solution was deaerated by purging with CO_2/CH_4 (1% CH_4, BOC gases) for 5 min. When two components were involved, the sensitizer (PdTPP, PdTPC, or $[Ru(Bpy)_3][PF_6]_2$) and the catalyst ($[Re(CO)_3(Pic)Bpy][PF_6]$) were present in equimolar concentrations. The solution was then irradiated, and the reactions were monitored by gas chromatography (GC), UV−vis, and gas infrared spectroscopies.

For GC analysis, a Unicam ProGC+ (ThermoONIX) fitted with a thermal conductivity detector was used. The gases, air, CO, CH_4, and CO_2, were separated with a Restek ShinCarbon ST 100/120 micropacked column (2 m, 1/16″ OD, 1.0 mm ID) fitted with "pigtails" of Restek intermediate-polarity deactivated guard column on either end (fused silica, 0.53 mm ID, 0.69 ± 0.05 mm OD). Ultra high purity He (N6.0, BOC gases) was used as the carrier gas and was passed through a GC triple carrier gas filter (Focus Technical) to remove trace impurities (oxygen, moisture, and hydrocarbons) prior to reaching the detector. Gas samples were injected manually (100 μL) using a Hamilton gastight locking syringe (500 μL). The amount of CO produced was quantified using a calibration plot. Known volumes of CO were mixed with a standard volume (large excess) of CO_2/1% CH_4. Samples were removed and analyzed by GC. The area of the CO peak was plotted versus the area of the CH_4 peak in the GC chromatogram. Moles of CO were calculated using the volume of an ideal gas (i.e., 22.4 L mol^{-1} at 293 K), and turnover numbers (TNs) of CO were calculated based on the moles of complex catalyst present in the reaction solution and the volume of cell headspace.

Crystallographic Structure Determination. The data for the crystallographic structure determination of $[\mathbf{Re(CO)_3(NCS)Bpy\text{-}PdTPP}]$ were collected on beamline I19 of the Diamond Light Source, using a Crystal Logic kappa geometry four-circle diffractometer equipped with a Rigaku Saturn 724+ CCD detector and a Cryostream cooler (at 120 K). The synchrotron X-ray wavelength was 0.68890 Å, selected by a Si(111) double-crystal monochromator at the Zr edge. The beam was focused by vertical and horizontal focusing mirrors. Rigaku CrystalClear software was used to record images.[44] Frame integration and unit-cell refinement were carried out with Bruker APEX2.[45] Absorption corrections were applied by SADABS (v2.03, Sheldrick). The structures were solved by direct methods using SHELXS-97 and refined by full-matrix least-squares using SHELXL-97.[46,47] Hydrogen atoms bound to carbon and nitrogen were placed at calculated positions and included in the refinement using a riding model. The benzene of crystallization was disordered and modeled over two sites with a refined relative occupancy of 80:20. The carbons of the benzene were modeled isotropically. Because of their close proximity, the pairs C(61a)/C(61b) and C(62a)/C(62)b were constrained to have identical ADP. The benzene was constrained to be hexagonal with a C−C distance of 1.39 Å. Crystallographic parameters are listed in Table 1.

Table 1. Unit Cell, Data Collection, and Refinement Parameters for $[\mathbf{Re(CO)_3(NCS)Bpy\text{-}PdTPP}]\cdot\mathbf{C_6H_6}$

formula	$C_{60}H_{37}N_8O_4PdReSC_6H_6$
Fw	1336.74
T (K)	120(2)
λ (Å)	0.68890
crystal system	triclinic
space group	$P\bar{1}$
a (Å)	9.401(2)
b (Å)	12.936(3)
c (Å)	23.410(5)
α (deg)	91.932(2)
β (deg)	94.160(2)
γ (deg)	105.874(3)
V (Å^3)	2726.9(10)
Z	2
ρ_{cald} (Mg/m^3)	1.628
μ (mm^{-1})	2.425
crystal color/shape	red/block
crystal size (mm^3)	0.04 × 0.04 × 0.02
θ range (deg)	0.85−24.16
no. of data	9300
no. of parameters	701
GOF	1.047
$R1$, $wR2$ (F^2, $I > 2\sigma(I)$)	0.0470, 0.1051
$R1$, $wR2$ (F^2, all data)	0.0734, 0.1151
CCDC no.	843937

Materials. NaNCS, AgOTf, $[Bu_4N][Br]$, $[H_4N][PF_6]$, aluminum oxide (activated acidic, Brockmann I), pyrrolidine (Aldrich), toluene, tetrahydrofuran (THF, Fisher), $Pd(OAc)_2$ (Alfa Aesar), *meso*-tetraphenylporphyrin (Frontier Scientific), and 3-picoline (BDH) were purchased commercially and used without further purification; NEt_3 (Aldrich) was dried over KOH or CaH_2 at room temperature and then distilled under argon; $[Ru(Bpy)_3]Cl_2\cdot 6H_2O$ (Aldrich) was converted to the PF_6^- salt ($[Ru(Bpy)_3][PF_6]_2$),[48] CH_2Cl_2 and DMF (Fisher) were dried on a solvent purification system and deaerated with argon prior to use. DMF was further dried over molecular sieves followed by distillation under argon. $Re(CO)_5Br$,[49] PdTPP,[37] Bpy-PdTPP,[37] $[Re(CO)_3(Pic)(Bpy)][PF_6]$,[29,37] *meso*-tetraphenylchlorin (TPC),[50,51] and 1-benzyl-1,4-dihydronicotinamide (BNAH)[52,53] were prepared according to literature methods. All other solvents and reagents were purchased commercially and used as received unless otherwise noted.

Synthesis of $[\mathbf{Re(CO)_3BrBpy\text{-}PdTPP}]$. This complex was synthesized as reported previously.[37] Since the compound was not fully characterized spectroscopically, we include a full set of data here.

^{1}H NMR (500 MHz, THF-d_8): δ 2.65 (3 H, s, Bpy CH_3); 7.55 (1 H, d, J 5.5 Hz, Bpy $H_{5'}$); 7.77 (9 H, m, 9 *m*-, *p*-phenyl); 8.14−8.20 (7

dx.doi.org/10.1021/ic200243y | Inorg. Chem. 2011, 50, 11877−11889

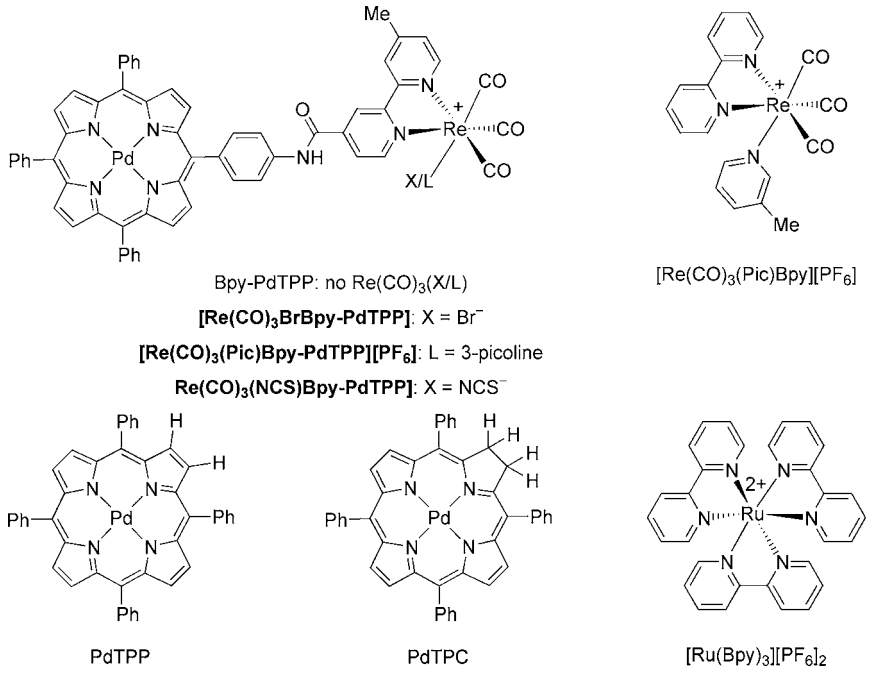

Figure 1. Chemical structures of complexes studied.

H, m, 6 *o*-phenyl, Bpy H_5); 8.20–8.25 (4 H, m, bridging C_6H_4); 8.67 (1 H, s, Bpy $H_{3'}$); 8.80 (4 H, s, *β*-pyrrolic H_a and H_b); 8.82 (2 H, d, *J* 5.0 Hz, *β*-pyrrolic H_c); 8.87 (2 H, d, *J* 5.0 Hz, *β*-pyrrolic H_d); 8.96 (1 H, d, *J* 5.5 Hz, Bpy $H_{6'}$); 9.04 (1 H, s, Bpy H_3); 9.29 (1 H, d, *J* 5.5 Hz, Bpy H_6); 10.36 (1 H, s, CONH). See the Supporting Information, Figure S2 for labeling of atoms.

IR(THF): ν(CO)/cm^{-1} 2020 (s), 1921 (s), 1897 (s).

ESI-MS (*m*/*z*): calcd for $[C_{59}H_{37}BrN_7O_4{}^{106}Pd^{187}Re]$ 1279.07; observed mass [M − Br + DMSO]$^+$ 1278.2 and [M − Br + MeCN]$^+$ 1241.2.

[Re(CO)$_3$(Pic)Bpy-PdTPP][PF$_6$]. [**Re(CO)$_3$(Pic)Bpy-PdTPP**]$^+$ was synthesized as the triflate salt,[37] and was converted to the PF_6^- salt by anion metathesis with $[H_4N][PF_6]$ in MeOH, and was isolated by precipitation with H_2O. The product was purified by column chromatography using silica gel 60 with CH_2Cl_2/THF (<10% THF) as the eluting solvent mixture.

^{1}H NMR (500 MHz, CD_2Cl_2): *δ* 2.28 (3 H, s, Bpy CH_3); 2.70 (3 H, s, 3-picoline CH_3); 7.28 (1 H, dd, *J* 7.7 and 5.9 Hz, 3-picoline H_5); 7.60 (1 H, d, *J* 5.7 Hz, Bpy $H_{5'}$); 7.68 (1 H, d, *J* 7.8 Hz, 3-picoline H_4); 7.75–7.81 (9 H, m, 9 *m*-, *p*-phenyl); 7.88 (1 H, d, *J* 5.6 Hz, 3-picoline H_6); 8.08 (1 H, s, 3-picoline H_2); 8.18–8.19 (6 H, m, *o*-phenyl); 8.21–8.25 (4 H, m, bridging C_6H_4); 8.35 (1 H, d, *J* 5.6 Hz, Bpy H_5); 8.50 (1 H, s, Bpy $H_{3'}$); 8.84 (4 H, s, *β*-pyrrolic H_a and H_b); 8.86 (2 H, d, *J* 4.9 Hz, *β*-pyrrolic H_c); 8.88 (1 H, s, Bpy H_3); 8.91 (2 H, d, *J* 4.9 Hz, *β*-pyrrolic H_d); 8.99 (1 H, d, *J* 5.7 Hz, Bpy $H_{6'}$); 9.28 (1 H, s, CONH); 9.33 (1 H, d, *J* 5.6 Hz, Bpy H_6). ^{31}P{^{1}H} NMR (202 MHz, CD_2Cl_2): *δ* −144.24 (septet, J_{P-F} 712.8 Hz, PF_6^-).

IR(THF): ν(CO)/cm^{-1} 2032 (s), 1928 (br s).

ESI-MS (*m*/*z*): calcd for $[C_{65}H_{44}N_8O_4{}^{106}Pd^{187}Re]^+$ 1293.2085; observed mass [M]$^+$ 1293.2050, difference 3.5 mDa.

[Re(CO)$_3$(NCS)Bpy-PdTPP]. A solution of [**Re(CO)$_3$BrBpy-PdTPP**] (0.084 mmol, 108 mg) was refluxed in the presence of excess NaNCS (9.37 mmol, 0.76 g) in THF (~25 mL) for 21 h under Ar. The cooled solution was diluted with saturated aqueous NaNCS (100 mL) and extracted with CH_2Cl_2 until no color remained in the aqueous layer. The combined CH_2Cl_2 portions were washed with H_2O (2 × 50 mL) and dried over $MgSO_4$. The CH_2Cl_2 solution was filtered, concentrated, and slow addition of hexane caused a precipitate to form that was collected by filtration. The crude product was purified by column chromatography using silica gel 60 with CH_2Cl_2 as the eluting solvent; 56 mg orange-red product recovered (53% yield). Single crystals suitable for X-ray diffraction were grown by layering a benzene solution of the complex with diethyl ether.

^{1}H NMR (500 MHz, CD_2Cl_2): *δ* 2.59 (3 H, s, Bpy CH_3); 7.52 (1 H, d, *J* 5.5 Hz, Bpy $H_{5'}$); 7.75–7.80 (9 H, m, 9 *m*-, *p*-phenyl); 8.17–8.18 (7 H, m, *o*-phenyl and Bpy H_5); 8.24–8.30 (4 H, m, bridging C_6H_4); 8.38 (1 H, s, Bpy $H_{3'}$); 8.73 (1 H, s, Bpy H_3); 8.84 (4 H, s, *β*-pyrrolic H_a and H_b); 8.86 (2 H, d, *J* 4.9 Hz, *β*-pyrrolic H_c); 8.89 (1 H, d, *J* 5.7 Hz, Bpy $H_{6'}$); 8.92 (2 H, d, *J* 4.9 Hz, *β*-pyrrolic H_d); 8.94 (1 H, s, CONH); 9.25 (1 H, d, *J* 5.5 Hz, Bpy H_6).

IR(THF): ν(CN)/cm^{-1} 2090 (br s); ν(CO)/cm^{-1} 2023 (s), 1922 and 1912 (s, overlapping peaks).

ESI-MS (*m*/*z*): calcd for $C_{60}H_{38}N_8O_4{}^{32}S^{106}Pd^{187}Re$ 1259.1329; observed mass [M + H]$^+$ 1259.1346; difference 1.7 mDa.

Palladium(II) *meso*-Tetraphenylchlorin (PdTPC). In a flask charged with TPC (>97% pure, 70 mg, 0.11 mmol) and $Pd(OAc)_2$ (54 mg, 0.24 mmol, 2.2 equiv) was added toluene (30 mL) and the suspension was refluxed (130 °C) under Ar for 18 h. The solvent was removed under vacuum, the dark purple residue redissolved in a minimum amount of CH_2Cl_2, and the solution passed through a plug of acidic alumina (to remove any unreacted free base TPC), rinsing with CH_2Cl_2 until the eluent was nearly colorless. The solution was concentrated, and addition of MeOH caused a dark purple precipitate to form, which was collected on a sintered glass funnel (note that filtrate still dark blue-green in color). The purple precipitate was very fine and difficult to handle; 50 mg recovered (63% yield), isolated in 92% purity, the remaining impurity was PdTPP as determined by ^{1}H NMR (Supporting Information,Figure S3).

^{1}H NMR (500 MHz, $CDCl_3$): *δ* 4.21 (4 H, s, pyrrolic C_2H_4); 7.60–7.69 (12 H, m, 8 *m*-, 4 *p*-phenyl); 7.80 (4 H, m, *o*-phenyl); 8.00 (6 H, m, 4 *o*-phenyl, 2 *β*-pyrrolic); 8.33 (4 H, m, *β*-pyrrolic).

PdTPP (for Comparison). ^{1}H NMR (500 MHz, $CDCl_3$): *δ* 7.72–7.79 (12 H, m, 8 *m*-, 4 *p*-phenyl); 8.17 (8 H, *o*-phenyl); 8.81 (8 H, s, pyrrolic).

RESULTS

Syntheses. The structures of the complexes studied here are shown in Figure 1. The cationic [**Re(CO)$_3$(Pic)Bpy-PdTPP**][**PF$_6$**] was synthesized from its [**Re(CO)$_3$BrBpy-PdTPP**] precursor,[37] followed by anion metathesis to the PF_6^- salt. In the earlier report [**Re(CO)$_3$BrBpy-PdTPP**] had not been characterized, but we have now done so using NMR,

dx.doi.org/10.1021/ic200243y | *Inorg. Chem.* 2011, 50, 11877–11889

Table 2. Selected Bond Lengths and Angles for $[Re(CO)_3(NCS)Bpy\text{-}PdTPP]\cdot C_6H_6$

		Bond Lengths (Å)	
Re(1)−N(6)	2.131(9)	Re(1)−N(7)	2.163(5)
Re(1)−N(8)	2.162(6)	Re(1)−C(58)	1.912(8)
Re(1)−C(59)	1.912(10)	Re(1)−C(60)	1.904(10)
C(58)−O(2)	1.158(9)	C(59)−O(3)	1.166(10)
C(60)−O(4)	1.168(10)	N(6)−C(57)	1.111(10)
C(57)−S(1)	1.639(10)	Pd(1)−N(1)	2.026(5)
Pd(1)−N(2)	2.019(5)	Pd(1)−N(3)	2.020(5)
Pd(1)−N(4)	2.011(5)		
		Bond Angles (deg)	
N(7)−Re(1)−N(8)	75.8(2)	C(58)−Re(1)−C(59)	87.5(3)
N(6)−Re(1)−C(60)	176.4(3)	C(58)−Re(1)−N(7)	172.9(3)
N(6)−Re(1)−N(8)	85.0(3)	N(6)−Re(1)−C(59)	92.7(3)
N(6)−C(57)−S(1)	176.2(8)	C(57)−N(6)−Re(1)	175.9(7)
N(1)−Pd(1)−N(3)	178.6(2)	N(2)−Pd(1)−N(4)	179.2(2)
N(1)−Pd(1)−N(2)	89.4(2)	N(2)−Pd(1)−N(3)	90.6(2)
		Torsion Angles (deg)	
C(40)−C(39)−C(6)−C(5)	119.4(7)	C(2)−C(1)−C(21)−C(22)	69.1(9)
C(22)−C(23)−C(24)−N(5)	178.1(7)	O(1)−C(27)−C(28)−C(32)	156.8(9)
C(32)−C(31)−C(33)−N(8)	179.2(7)		

UV−vis, and IR spectroscopies, and mass spectrometry. It is worth noting that in the mass spectrum only solvent complexes of $[Re(CO)_3BrBpy\text{-}PdTPP]$ could be observed, namely, $[Re(CO)_3(DMSO)Bpy\text{-}PdTPP]^+$ and $[Re(CO)_3(MeCN)\text{-}Bpy\text{-}PdTPP]^+$.

The free base TPC was prepared[50] and isolated[51] by modified literature methods. Palladium(II) was then inserted by refluxing TPC with excess $Pd(OAc)_2$ to give PdTPC. Because of trace amounts of *meso*-tetraphenylporphyrin (TPP) impurity in the isolated TPC (<3%), we were only able to obtain purity up to 92% (based on ^1H NMR) of PdTPC, the only impurity being PdTPP (See the Supporting Information, Figure S3). Insertion of Pd(II) into TPC required longer periods of refluxing relative to the corresponding insertion into TPP. To the best of our knowledge the only studies of PdTPC described either (i) methods used to determine complex purity,[54] (ii) association properties in aqueous solution,[55] or (iii) triplet emission quenching under various conditions.[56−59] The latter reports by Sapunov and co-workers dealt with effects on triplet emission quenching that included concentration dependence in aqueous[56] and organic media,[57] quenching by heme proteins and cyanocobalamin,[58] and the triplet state emission quenching of PdTPP by PdTPC in toluene.[59]

Crystallography. After several unsuccessful attempts at growing single crystals of $[Re(CO)_3(Pic)Bpy\text{-}PdTPP][PF_6]$ and $[Re(CO)_3BrBpy\text{-}PdTPP]$, we instead synthesized $[Re(CO)_3(NCS)Bpy\text{-}PdTPP]$ by reaction of $[Re(CO)_3BrBpy\text{-}PdTPP]$ with NaNCS. Its X-ray structure was determined from data collected at the Diamond synchrotron because of the small size of the crystals (Table 2, Figure 2). The Re(I) center has a geometry representative of the analogous mononuclear $[Re(CO)_3(NCS)(Bpy)]$ complex reported by Vlček, and co-workers.[60] The three CO ligands are in a *facial* arrangement around the Re(I) center with near 90° angles between ligands, while the N(7)−Re(1)−N(8) Bpy bite angle is comparatively smaller at 75.8(2)°. As reported for the mononuclear $[Re(CO)_3(NCS)(Bpy)]$,[60] the Re−N(CS) bond in $[Re(CO)_3(NCS)Bpy\text{-}PdTPP]$ is angled slightly, only about 4°, toward the chelating Bpy ligand.

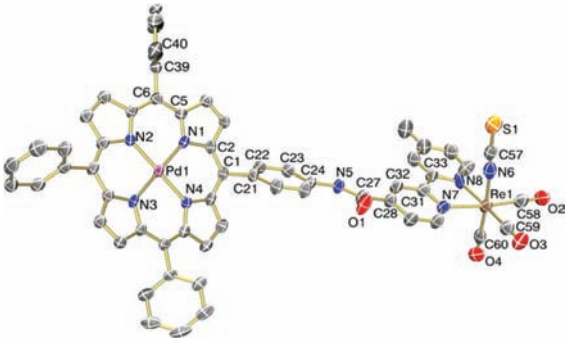

Figure 2. ORTEP drawing of $[Re(CO)_3(NCS)Bpy\text{-}PdTPP]\cdot C_6H_6$; hydrogen atoms and C_6H_6 solvent molecule omitted for clarity. Anisotropic displacement parameters shown at 50% probability.

The chromophoric porphyrin constituent of $[Re(CO)_3(NCS)Bpy\text{-}PdTPP]$ adopts a square planar geometry at the Pd(II) nucleus having N−Pd−N bond angles of nearly 90 and 180°, and is comparable to the structure of PdTPP, reported in 1964 by Fleischer et al.[61] The overall porphyrin moiety is nonplanar in both $[Re(CO)_3(NCS)Bpy\text{-}PdTPP]$ and mononuclear PdTPP. The nonplanar porphyrin in $[Re(CO)_3(NCS)Bpy\text{-}PdTPP]$ forms a saddle with pairs of opposite β-carbons. For example, C(3) and C(4) paired with C(13) and C(14) make up the high point of the saddle, while C(8) and C(9) paired with C(18) and C(19) make up the low point of the saddle. In contrast, the saddle structure in mononuclear PdTPP has the *meso*-carbons of the porphyrin backbone as the highest and lowest points in the saddle.[61]

Also of interest in the structure of $[Re(CO)_3(NCS)Bpy\text{-}PdTPP]$ is the planarity of the phenylamide link between porphyrin and Re(I)Bpy. Should the two components of the dyad arrange in a planar conformation, this will optimize electron transfer efficiency from chromophore to catalyst. As it turns out, the phenylamide linker is nearly planar in itself with the C(22)−C(23)−C(24)−N(5) torsion angle being 178.1(7)°, but is out of the plane of the porphyrin (C(2)−C(1)−C(21)−C(22)) by 69.1(9)° and is out of the plane of

dx.doi.org/10.1021/ic200243y | Inorg. Chem. 2011, 50, 11877−11889

the Re(I)Bpy with the O(1)−C(27)−C(28)−C(32) torsion angle at 156.8(9)°.

Steady-State Photochemistry. Selective excitation of the [**Re(CO)$_3$(Pic)Bpy-PdTPP**][**PF$_6$**] porphyrin core (λ > 495 nm) induces remote-site substitution of 3-picoline at the Re(I)Bpy center.[37] This extraordinary photoreaction can be observed using steady-state IR spectroscopy under a variety of conditions in the presence of the sacrificial electron donor, NEt_3. For example, in THF, DMF, or butyronitrile solution with an added nucleophilic bromide source, 3-picoline is substituted by bromide at the Re(I)Bpy center forming neutral [**Re(CO)$_3$BrBpy-PdTPP**]. In the absence of bromide, 3-picoline is instead substituted by a solvent molecule such as DMF, NEt_3, THF, and so forth. Alternatively, in the presence of 1% excess 3-picoline in THF, the rapid formation of a radical species, believed to be [**Re$^+$(CO)$_3$(Pic)Bpy$^-$-PdTPP**], can be detected in the solution IR spectrum with ν(CO) at 2011, 1907, and 1893 cm^{-1}.[37]

Loss of the labile ligand bound to Re(I)Bpy, 3-picoline in the current study, is one of the steps that is known to take place during the catalytic cycle of the photoreduction of CO_2 by mononuclear Re(I) tricarbonyl diimine complexes.[3,17,18] It is therefore important to know the efficiency with which this reaction proceeds, particularly in DMF solution, as it is the solvent of choice for photochemical CO_2 reduction systems that employ such catalysts.[25] A solution of [**Re(CO)$_3$(Pic)Bpy-PdTPP**][**PF$_6$**] in DMF/NEt_3 (5:1 v/v) with 0.12 M [Bu_4N][Br] was irradiated with a narrow bandwidth filter (λ_{ex} = 520 nm), forming [**Re(CO)$_3$BrBpy-PdTPP**] quantitatively in less than 6 min.[62] During the photoreaction, the UV−vis absorbance changes by approximately 5% from time zero, until the reaction is finished. In contrast to the small changes in the UV−vis absorbance, the changes in the infrared spectrum are substantial and there is almost no peak overlap between [**Re(CO)$_3$(Pic)Bpy-PdTPP**][**PF$_6$**] and [**Re(CO)$_3$BrBpy-PdTPP**]. Because of this, the quantum yield was obtained from changes in the infrared spectra over time (see Figure 3).[62]

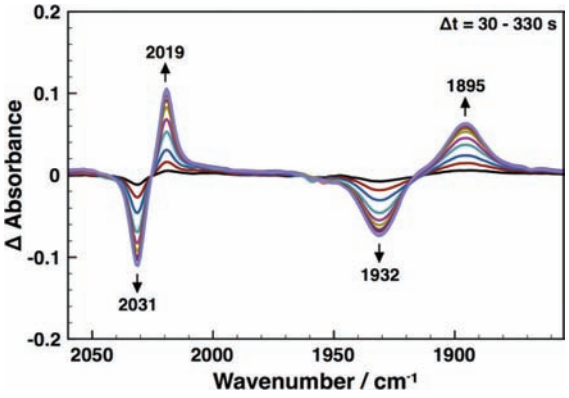

Figure 3. Difference IR spectra for the steady-state photosubstitution reaction of [**Re(CO)$_3$(Pic)Bpy-PdTPP**][**PF$_6$**] measured at intervals from 30 s up to 330 s, showing the replacement of 3-picoline by bromide in DMF/NEt_3 (5:1 v/v) with 0.12 M [Bu_4N][Br] and λ_{ex} = 520 nm.

The kinetic models of the infrared absorbances at 2031 and 2019 cm^{-1} are shown in the Supporting Information, Figure S4.

Photoreduction of CO_2. *[Re(CO)$_3$(Pic)Bpy-PdTPP][PF$_6$] as a Molecular Photocatalyst.* The molecular dyad [**Re(CO)$_3$(Pic)Bpy-PdTPP**][**PF$_6$**] was designed to lower the energy required to sensitize the photocatalytic reduction of CO_2 to CO with a molecular Re(I) tricarbonyl diimine catalyst. The dyad was tested for photocatalytic CO_2 reduction using literature conditions (see Introduction) that entail steady-state photolysis of the complex in DMF/NEt_3 (5:1 v/v) solution saturated with CO_2. We employ NEt_3 as a sacrificial electron donor to maintain consistency with other steady-state and time-resolved studies. The photoreduction reaction was monitored by gas chromatography, UV−vis spectroscopy, and in some instances solution IR spectroscopy. The photolysis cell used in each reaction was connected to a infrared gas cell (Supporting Information, Figure S1), and the gas-phase IR spectra were measured before and after photolysis to further monitor the formation of CO. This was especially useful during photoreactions where only small amounts of CO could be observed, as gas-phase IR spectroscopy was a more sensitive technique than gas chromatography under the conditions in this study.

In the case of [**Re(CO)$_3$(Pic)Bpy-PdTPP**][**PF$_6$**], only 2 turnovers of CO could be observed with λ > 420 nm (porphyrin S_2 excitation), and only trace amounts using λ > 495 nm (porphyrin S_1) excitation. In all experiments with a steady-state method, UV−vis spectroscopy detects the formation of a new porphyrin photoreduction product *or* products, one of which has an absorption maximum of 603 nm and can be identified as a chlorin species (Supporting Information, Figure S5). This observation is consistent with a report by Whitten and co-workers that described the formation of chlorin and *iso*-bacteriochlorin reduction products of PdTPP when photolyzed in the presence of dimethylaniline (DMA).[63] In that study, one C−C bond of the pyrrole ring (or rings for *iso*-bacteriochlorin) was thought to be hydrogenated in one position and aminated at the other carbon through one of the methyl groups of the DMA.

With narrow bandwidth excitation (λ_{ex} = 520 nm) of [**Re(CO)$_3$(Pic)Bpy-PdTPP**][**PF$_6$**], only minimal amounts of chlorin are formed within 4 h (absorbance ∼0.1, Supporting Information, Figure S5), but more grows in with longer photolysis times (absorbance >1). No CO is observed after 4 h of photolysis with λ_{ex} = 520 nm and only trace amounts are observed after 8 h, with no increase up to 21 h photolysis.

With a 420 nm cutoff filter, 2 TNs CO can be obtained after 4 h, but the onset of CO formation occurs only at 2 h, and the reaction is complicated by the competing photoreduction products of the porphyrin core. To probe the Re(I)Bpy part of the dyad, the solution IR spectra were measured after photolysis showing ν(CO) at 2017, 1908, and about 1891 cm^{-1}, suggesting the formation of a formate complex, [**Re(CO)$_3$(OCHO)Bpy-PdTPP**]. The proposal of a formate complex is based on a study by Fujita and co-workers, where the reaction of Re(CO)$_3$(dmb), a reduced form of [Re(CO)$_3$(OTf)(dmb)], with CO_2 yielded [Re(CO)$_3$(OCHO)(dmb)] (dmb = 4,4′-dimethyl-2,2′-bipyridine) and was reported to have ν(CO) at 2017, 1911, and 1888 cm^{-1} in DMF solution.[19] The IR spectrum demonstrates that while the Pd(II) porphyrin core is being reduced, the Re(I)Bpy site undergoes photosubstitution of 3-picoline by other species present in solution (Table 3).

Two-Component Photoreduction System. In light of the observation of chlorin formation using [**Re(CO)$_3$(Pic)Bpy-PdTPP**][**PF$_6$**], we hypothesized that the chlorin may be a better photosensitizer than the porphyrin. To test this idea we synthesized PdTPC, the hydrogenated porphyrin derivative of PdTPP, and employed mixtures of two components, sensitizer

dx.doi.org/10.1021/ic200243y | Inorg. Chem. 2011, 50, 11877−11889

Table 3. UV-vis and Emission Data for Selected Complexes

complex	λ_{abs}/nm (ε/10^3 dm^3 mol^{-1} cm^{-1})	λ_{em}/nm [d]
[**Re(CO)$_3$BrBpy-PdTPP**] [a]	417 (249), 484 (3.8), 524 (23.6), 554 (2.3)	565, 610, *705*, 775
[**Re(CO)$_3$(Pic)Bpy-PdTPP**][**PF$_6$**] [a]	416 (275), 484 (3.7), 524 (31.2), 554 (2.7)	565, 610, *705*, 775
PdTPP [b]	416 (314), 463 (2.7), 485 (3.3), 523 (31.3), 554 (2.8)	563, 612, *706*, 775
PdTPC [c]	410 (192), 496 (6.6), 529 (4.9), 563 (10.0), 603 (55.0)	614, 659, *794*

[a]Measured in THF, λ_{ex} = 524 nm. [b]Measured in CH_2Cl_2, λ_{ex} = 524 nm. [c]Measured in CH_2Cl_2, λ_{ex} = 603 nm. [d]Emission maximum marked in italics.

and [Re(CO)$_3$(Pic)Bpy][PF$_6$], for CO_2 reduction. When comparing the TNs of all the systems, the system with PdTPC as the sensitizer was generally more effective in the photoreduction of CO_2 to CO (Figure 4). However, only when

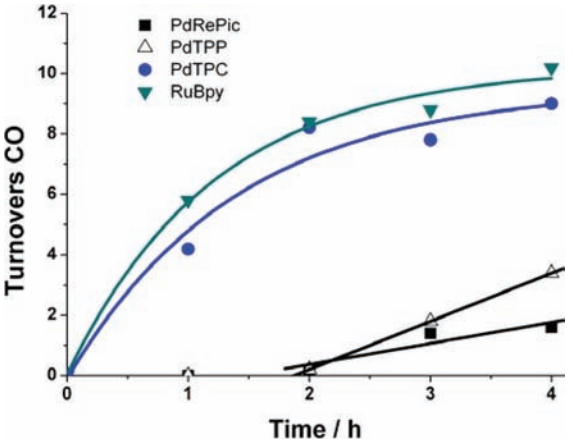

Figure 4. Turnovers of CO obtained from steady-state photolysis in DMF/NEt$_3$ (5:1 v/v) solution saturated with CO_2; complexes 0.05 mM except [**Re(CO)$_3$(Pic)Bpy-PdTPP**][**PF$_6$**] (0.27 mM); λ > 420 nm except [Ru(Bpy)$_3$][PF$_6$]$_2$ (λ > 495 nm); PdTPP, PdTPC, and [Ru(Bpy)$_3$][PF$_6$]$_2$ are 1:1 two-component mixtures with [Re(CO)$_3$(Pic)Bpy][PF$_6$]. PdRePic = [**Re(CO)$_3$(Pic)Bpy-PdTPP**][**PF$_6$**], RuBpy = [Ru(Bpy)$_3$][PF$_6$]$_2$.

exciting into the S_2 state did the system produce moderate amounts of CO.[64] To further complicate matters, S_2 excitation of PdTPC results in quantitative chlorin photoreduction to a bacteriochlorin species (Q-band λ_{abs}^{max} = 588 nm), as evidenced by steady-state UV−visible spectroscopy[50,51] (Supporting Information, Figure S6), while S_1 excitation of PdTPC gives only minimal amounts of bacteriochlorin (ΔAbs ~0.4). For comparison, the two-component system with tris(bipyridine) ruthenium(II) ([Ru(Bpy)$_3$][PF$_6$]$_2$) and [Re(CO)$_3$(Pic)Bpy][PF$_6$] was also studied and proved to be more effective than either of the two-component systems with PdTPP or PdTPC sensitizers (Figure 4).

Ground State Spectroscopy. *UV−vis Absorption Spectra.* The UV−vis absorption spectrum of [**Re(CO)$_3$(Pic)Bpy-PdTPP**][**PF$_6$**] in THF solution matches that reported previously,[37] and it completely masks the absorption spectrum of mononuclear [Re(CO)$_3$(Pic)Bpy][PF$_6$], even at low concentrations (Supporting Information, Figure S7). There is no discernible difference in the electronic spectra of Bpy-PdTPP, [**Re(CO)$_3$BrBpy-PdTPP**], and [**Re(CO)$_3$(Pic)Bpy-PdTPP**][**PF$_6$**]. The mononuclear sensitizer PdTPC has a distinctly different UV−vis absorption spectrum from that of PdTPP (Supporting Information, Figure S8). While PdTPP portrays a similar electronic spectrum to [**Re(CO)$_3$(Pic)Bpy-PdTPP**][**PF$_6$**] with a Q-band absorption maximum at 523 nm in CH_2Cl_2 solution (ε = 31 300 M^{-1} cm^{-1}), the Q-band maximum of PdTPC is red-shifted significantly to 603 nm and has a higher extinction coefficient, ε = 55 000 M^{-1} cm^{-1}, as well as another notable Q-band at 563 nm with ε = 10 000 M^{-1} cm^{-1} (Table 3). Not only are the Q-peaks shifted substantially, but PdTPC possesses lower symmetry than PdTPP, C_{2v} versus D_{4h}, respectively.

Emission Spectroscopy. The steady-state emission spectra of Bpy-PdTPP, [**Re(CO)$_3$BrBpy-PdTPP**], and [**Re(CO)$_3$(Pic)Bpy-PdTPP**][**PF$_6$**] in THF solution (λ_{ex} = 524 nm) are shown in Supporting Information, Figure S7. The complexes exhibit weak singlet emission at 565 and 610 nm and strong triplet emission at 705 and 775 nm, assigned to $^1Q_{0,0}$ (or E_{00}) and $^1Q_{1,0}$ and $^3Q_{0,0}$ and $^3Q_{1,0}$ transitions, respectively, with E_{00} determined to be 2.19 eV for all three complexes. It is noteworthy that at equimolar concentrations the emission intensities of Bpy-PdTPP and [**Re(CO)$_3$BrBpy-PdTPP**] remain unchanged while that of the cationic [**Re(CO)$_3$(Pic)Bpy-PdTPP**][**PF$_6$**] is quenched by 37%. This is in contrast to our earlier report in butyronitrile solution where we observed no change in the emission intensity of [**Re(CO)$_3$(Pic)Bpy-PdTPP**][**OTf**] relative to Bpy-PdTPP, nor the $^3Q_{1,0}$ transition.[37]

The steady-state emission spectra of PdTPP and PdTPC in CH_2Cl_2 solution are shown in Supporting Information, Figure S9. The emission profile of PdTPP (λ_{ex} = 524 nm, CH_2Cl_2) is very similar to that of the Pd(II) porphyrins in THF solution, having weak singlet emission at 563 and 612 nm and strong triplet emission at 706 and 775 nm (E_{00} = 2.20 eV). The emission quenching of PdTPP by NEt$_3$ in CH_2Cl_2 solution was found to follow Stern−Volmer behavior ($M_0/M = 1 + K_{SV}[Q]$, where $K_{SV} = k_q t_0$) and has a Stern−Volmer constant of K_{SV} = 24 M^{-1} (Supporting Information, Figure S10). The emission of PdTPC is less trivial than that of PdTPP. First, the emission intensity of PdTPC relative to PdTPP is significantly lower. Excitation of PdTPC at 603 nm in CH_2Cl_2 gives an emission maximum at 794 nm and two weaker bands at 614 and 659 nm. These have been tentatively assigned to the $^3Q_{0,0}$, $^1Q_{0,0}$, and $^1Q_{1,0}$ transitions, respectively. Supporting Information, Figure S11 shows the emission spectra of PdTPC excited at different wavelengths, 524, 560, and 603 nm, all of which give the same emission profile. With the assumption that the band at 614 nm is the $^1Q_{0,0}$ transition, PdTPC has an E_{00} of 2.02 eV, lower by 0.18 eV than that of PdTPP. One could argue that the band at 614 nm is merely due to the 8% PdTPP impurity. If this were the case we would expect to see triplet emission from PdTPP as well, which was not observed.

Electrochemistry. The oxidation and reduction potentials of [**Re(CO)$_3$(Pic)Bpy-PdTPP**][**PF$_6$**], PdTPP, and PdTPC were determined by cyclic voltammetry in CH_2Cl_2 solution with 0.1 M [Bu$_4$N][PF$_6$], and are reported versus the ferrocenium/ferrocene couple ($Fc^{+/0}$), which was used as an internal standard in all experiments (Table 4). The cyclic voltammograms for [**Re(CO)$_3$(Pic)Bpy-PdTPP**][**PF$_6$**] and PdTPC are shown in Supporting Information, Figure S12. In

dx.doi.org/10.1021/ic200243y | Inorg. Chem. 2011, 50, 11877−11889

Table 4. Redox Potentials and Free Energy Change (ΔG_{ox}*) for *Intra-* and *Inter*molecular Electron Transfer from Pd(II) Porphyrin/Chlorin S_1 Excited States to Re(I)Bpy Moieties

complex[a]	$E_{1/2}^{ox}$/V (ΔE/mV)	$E_{1/2}^{red}$/V (ΔE/mV)	ΔG_{ox}*[b]/eV
[Re(CO)$_3$(Pic)Bpy-PdTPP][PF$_6$]	+0.63 (66)	−1.48 (90)	−0.08
PdTPP	+0.65 (95)	−1.81 (136)	+0.02
PdTPC	+0.34 (55)	−1.79 (100)	−0.17
[Re(CO)$_3$(Pic)Bpy][PF$_6$]		−1.57 (99)	

[a]Measured in CH_2Cl_2 with 0.1 M [Bu$_4$N][PF$_6$] and $Fc^{+/0}$ as internal standard; 100 mV/s scan rate. [b]Calculated from ΔG_{ox}* = $E_{1/2}^{ox}$ − $E_{1/2}^{red}$ − E_{00}.

the experimental window, all complexes show one reversible oxidation and one reversible reduction. **[Re(CO)$_3$(Pic)Bpy-PdTPP][PF$_6$]** and PdTPP exhibit similar oxidation potentials at +0.63 and +0.65 V, respectively, that are smaller than the converted literature values for PdTPP (+0.74 V vs $Fc^{+/0}$ but measured under different conditions).[65] PdTPC, having one of its pyrrole rings fully hydrogenated, is predictably easier to oxidize (+0.34 V) than either of the former complexes. Conversely, the reduction potentials of PdTPP and PdTPC are similar at −1.81 and −1.79 V, respectively, while that of **[Re(CO)$_3$(Pic)Bpy-PdTPP][PF$_6$]** at −1.48 V resembles the zinc analogue, **[Re(CO)$_3$(Pic)Bpy-ZnTPP][OTf]** (−1.44 V vs $Fc^{+/0}$), yet differs from [Re(CO)$_3$(Pic)Bpy][PF$_6$] by 0.09 V (Table 4). In an earlier study, we compared the reduction potentials of **[Re(CO)$_3$(Pic)Bpy-ZnTPP][OTf]** to that of a rhenium complex functionalized with an 4-*t*Bu-phenyl amido unit to mimic the effect of the linker (the diimine ligand was 4-methyl-2,2′-bipyridine-4′-carboxyamid-(4-*t*Bu-phenyl)yl).[35] Their potentials were −1.44 and −1.45 V vs $Fc^{+/0}$ in THF showing that the amidophenyl group makes the Re(Bpy) moiety easier to reduce.

Considering that the oxidations in **[Re(CO)$_3$(Pic)Bpy-PdTPP][PF$_6$]**, PdTPP, and PdTPC are based on the macrocycle it is expected that the PdTPC, being saturated at one pyrrole ring, would be easier to oxidize. The reduction in **[Re(CO)$_3$(Pic)Bpy-PdTPP][PF$_6$]** is localized on the bipyridine ligand bound to Re(I) and thus has a reduction potential similar to its analogous Zn dyad and to that of the mononuclear [Re(CO)$_3$(Pic)Bpy][PF$_6$], also having a first reduction on the bipyridine ligand.[66] These results again emphasize the lack of interaction between metalloporphyrin (Pd or Zn) sensitizer and Re(I)Bpy in the ground state.

Estimation of Driving Force (ΔG_{ox}*). From cyclic voltammetry and steady-state emission experiments it is possible to estimate the free energy change (ΔG_{ox}*) for *intra*molecular photoinduced electron transfer from Pd(II) porphyrin S_1 excited-state to Re(I)Bpy in the **[Re(CO)$_3$(Pic)Bpy-PdTPP][PF$_6$]** molecular dyad using the simplified eq 1.

$$\Delta G_{ox}^{*} = E_{ox} - E_{red} - E_{00} \quad (1)$$

where E_{ox} and E_{red} are taken to be +0.63 and −1.48 V, respectively, and E_{00} is 2.19 eV. While E_{00} is commonly estimated from the highest energy emission maximum in a frozen glass sample,[67] a structured emission spectrum of **[Re(CO)$_3$(Pic)Bpy-PdTPP][PF$_6$]** can be obtained at room temperature. The value for E_{00} was therefore estimated from the singlet emission band ($^1Q_{0,0}$) of **[Re(CO)$_3$(Pic)Bpy-PdTPP][PF$_6$]** at 565 nm (Supporting Information, Figure S7). Thus ΔG_{ox}* was calculated to be slightly favorable at −0.08 eV. This differs to a small degree from our earlier report, ΔG_{ox}* = −0.03 eV, but that calculation was performed using literature values for PdTPP.[37] This favorable electron transfer process is also supported by the steady-state emission spectrum (Supporting Information, Figure S7), where we observed the intensity of the emission of **[Re(CO)$_3$(Pic)Bpy-PdTPP][PF$_6$]** to be quenched by 37% relative to Bpy-PdTPP (no Re(I)) and **[Re(CO)$_3$BrBpy-PdTPP]** (neutral overall charge). It is also noteworthy that *intra*molecular transfer from the Pd(II) porphyrin T_1 excited-state to Re(I)Bpy is a thermodynamically uphill process, having ΔG_{ox}* = +0.35 eV (E_{00} for T_1 is 1.76 eV).

To estimate ΔG_{ox}* for *inter*molecular transfer from PdTPP or PdTPC to [Re(CO)$_3$(Pic)Bpy][PF$_6$] we simply use the E_{red} potential of mononuclear [Re(CO)$_3$(Pic)Bpy][PF$_6$] (−1.57 V) in eq 1. By doing so, we obtain ΔG_{ox}* values of +0.02 and −0.17 eV for PdTPP and PdTPC, respectively. Thus *inter*molecular electron transfer from PdTPC to [Re(CO)$_3$(Pic)Bpy][PF$_6$] appears to be a thermodynamically favorable process, but ΔG_{ox}* for *inter*molecular electron transfer from PdTPP to [Re(CO)$_3$(Pic)Bpy][PF$_6$] was estimated to be nearly zero. It also follows that the thermodynamic driving force for *inter*molecular electron transfer from the sensitizer triplet state to catalyst is an uphill process, having ΔG_{ox}* = +0.46 eV (E_{00} = 1.76 eV) for PdTPP:[Re(CO)$_3$(Pic)Bpy][PF$_6$], and ΔG_{ox}* = +0.35 eV (E_{00} = 1.56 eV) for PdTPC:[Re(CO)$_3$(Pic)Bpy][PF$_6$].

Picosecond Time-Resolved Infrared Spectroscopy (ps-TRIR). We have investigated the photophysics of **[Re(CO)$_3$(Pic)Bpy-PdTPP][PF$_6$]** using ps-TRIR spectroscopy since this approach probes the initial photoprocesses, and is a powerful technique for interrogating *intra*molecular energy or electron transfer in multinuclear complexes.[68−70]

Irradiation (λ_{ex} = 532 nm) of a solution of **[Re(CO)$_3$(Pic)Bpy-PdTPP][PF$_6$]** in CH_2Cl_2 leads to the production of three transient ν(CO) bands at lower energy relative to those of the parent complex at 2029, 2008, and 1908 cm^{-1} (Figure 5). The

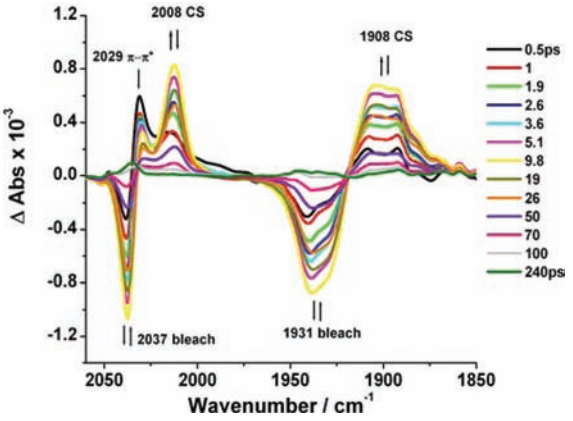

Figure 5. Picosecond TRIR spectra of **[Re(CO)$_3$(Pic)Bpy-PdTPP][PF$_6$]** in CH_2Cl_2 (λ_{ex} = 532 nm); bleach is due to the depletion of the ground state complex, while π–π* and charge-separated (CS) are bands from excited states of the complex. Notice the positive bands overlapping the bleach (see 100 and 240 ps spectra), leading to its apparent reformation.

transient band at 2029 cm^{-1} rises on a subpicosecond time scale while the bands at 2008 and 1908 cm^{-1} grow in with a

dx.doi.org/10.1021/ic200243y | Inorg. Chem. 2011, 50, 11877–11889

lifetime of about 3 ps (Figure 6). The three transient bands are found to decay fully (τ_{decay} ~30 ps) with concomitant

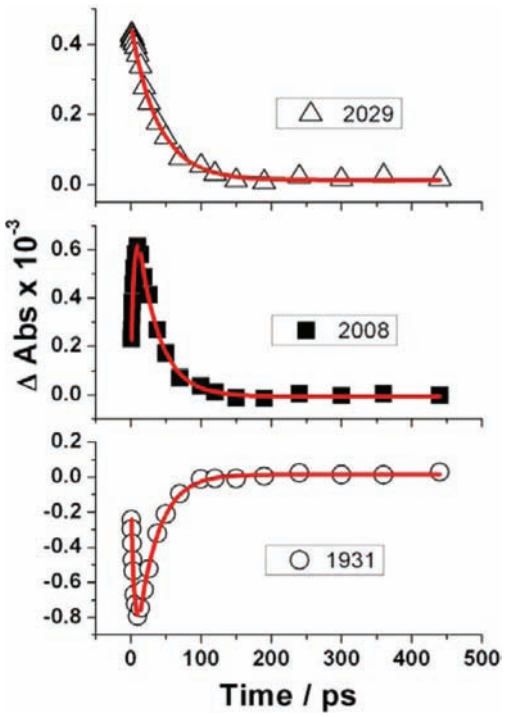

Figure 6. Kinetic traces for selected bands in the ps-TRIR experiment shown in Figure 5 for [**Re(CO)$_3$(Pic)Bpy-PdTPP**][**PF$_6$**] in CH_2Cl_2 solution (λ_{ex} = 532 nm). The triangles, solid squares, and circles show experimental points. The continuous lines show the best-fit lines.

formation of two new bands at 2035 and 1935 cm^{-1}, which overlap with the parent bleaches, leading to its apparent reformation (see the 100 and 240 ps traces in Figure 5).[71]

When sacrificial electron donor NEt_3 (1 M) is added to the solution, the same transient bands are observed but these display different kinetic lifetimes. The species at 2029 cm^{-1} still rises on a subpicosecond time scale but the other two bands at 2008 and 1908 cm^{-1} *grow* two times more slowly (ca. 6 ps) than in the absence of NEt_3. The *decay* of the band at 2029 cm^{-1} occurs faster than in the absence of NEt_3 (ca. 20 vs 30 ps, respectively). Conversely, the bands at 2008 and 1905 cm^{-1} *decay* more slowly than in the absence of NEt_3 (ca. 45 vs 30 ps). Again, two new ν(CO) bands are observed to form which overlap the parent bleaches, upon decay of the transients.

Nanosecond Time-Resolved Infrared Spectroscopy (ns-TRIR). Experiments were performed on the nanosecond time scale in an attempt to observe the catalytically active species which leads to photosubstitution of Pic by bromide. Excitation of [**Re(CO)$_3$(Pic)Bpy-PdTPP**][**PF$_6$**] in CH_2Cl_2 with a 532 nm laser, leads to the formation of two new positive ν(CO) bands overlapping the parent, which correspond to those observed in the latter stages of the ps-TRIR experiments. These bands decay with a lifetime of ~1 μs, leading to the apparent rebleaching of the parent, and the formation of two additional bands at 2008 and 1903 cm^{-1}. The bands at 2008 and 1903 cm^{-1} have a lifetime of 10 μs, which matches the recovery of the ground-state complex at 2032 and 1931 cm^{-1}. Repeating these measurements in the presence of 1 M NEt_3 leads to identical spectra, but with significantly different kinetic behavior, Figures 7 and 8. The transient bands

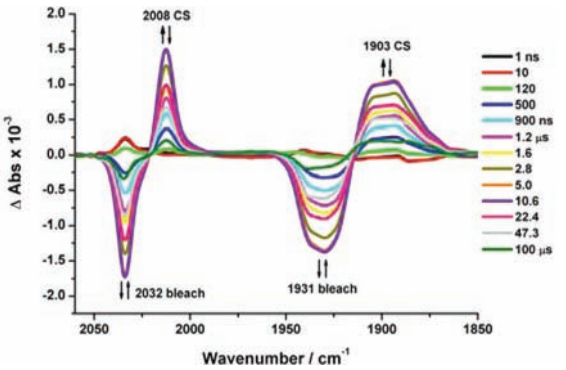

Figure 7. Nanosecond TRIR spectra of [**Re(CO)$_3$(Pic)Bpy-PdTPP**][**PF$_6$**] in CH_2Cl_2 with 1 M NEt_3 (λ_{ex} = 532 nm); bleach is due to the depletion of the ground state complex, and CS indicates a charge-separated excited-state complex. Notice the positive bands overlapping the bleach (see 1, 10, and 120 ns spectra), which correspond to those observed in the latter stages of the ps-TRIR experiments.

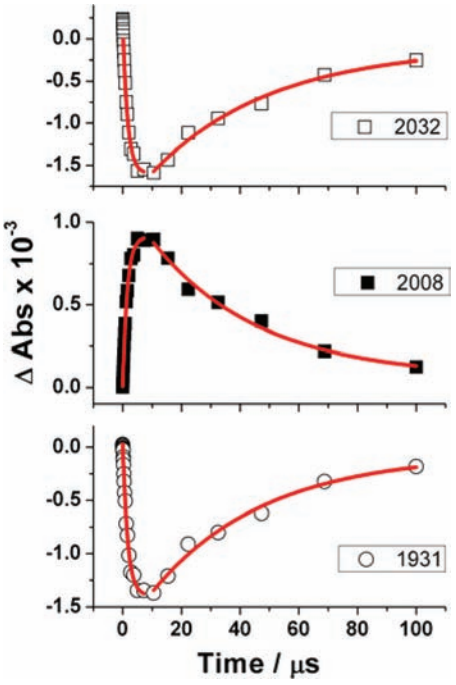

Figure 8. Kinetic traces for selected bands in the ns TRIR experiment shown in Figure 7 for [**Re(CO)$_3$(Pic)Bpy-PdTPP**][**PF$_6$**] in CH_2Cl_2 solution with 1 M NEt_3 (λ_{ex} = 532 nm). The squares, solid squares, and circles show experimental points. The continuous lines show the best-fit lines.

at 2008 and 1903 cm^{-1} now grow in and decay more slowly than in the absence of NEt_3 (τ_{growth} ~ 2 μs; τ_{decay} ~ 45 μs), and these rates closely match those of the parent rates of recovery.

Even with the experiments described above, there is still a need to link the ns-TRIR and the steady-state remote-site photosubstitution reactions, and we have used a combination of microsecond TRIR and rapid-scan FTIR spectroscopies to probe this further. We found that a single laser shot (λ_{ex} = 532 nm) on a solution of [**Re(CO)$_3$(Pic)Bpy-PdTPP**][**PF$_6$**] in CH_2Cl_2 in the presence of NEt_3 (1 M) and [Bu_4N][Br] (0.1 M) leads to identical results to those obtained in the fast ns-TRIR experiments. No evidence for growth of the substituted bromide complex, [**Re(CO)$_3$BrBpy-PdTPP**], was obtained during this experiment (Supporting Information, Figure S13).

dx.doi.org/10.1021/ic200243y | *Inorg. Chem.* 2011, 50, 11877–11889

However, when the same solution was subjected to pulsed laser shots for 3 s at 10 Hz, a long-lived product is observed (ν(CO) 2010 and 1900 cm^{-1}) which may indicate formation of a one-electron reduced (OER) species (Supporting Information, Figure S13). Monitoring this reaction with rapid-scan FTIR allows us to measure the rate of substitution of Pic by bromide. The decay of this species is the same as the growth of the bromide product, **[Re(CO)$_3$BrBpy-PdTPP]** (k_{obs} = 0.12 (±0.01) s^{-1}) (Supporting Information, Figure S13).

DISCUSSION

[Re(CO)$_3$(Pic)Bpy-PdTPP][PF$_6$]: CO$_2$ Reduction in Perspective. We first compare **[Re(CO)$_3$(Pic)Bpy-PdTPP][PF$_6$]** to other dyads, but we note that quantitative comparisons are not possible without using the same experimental conditions (i.e., solvent system, sacrificial reagent, light source, reaction vessel, etc.).

Dyads that contain Ru(Bpy)$_3^{2+}$, or derivatives thereof, as the photosensitizer component are by far the most studied complexes toward the photochemical reduction of CO_2 to CO. Kimura et al. first reported three such dyads with the sensitizer linked to a Ni(cyclam)$^{2+}$ (cyclam = 1,4,8,11-tetraazacyclotetradecane) catalyst.[72,73] While Ni(cyclam)$^{2+}$ is a highly selective electrocatalyst for CO_2 reduction to CO,[74] the molecular dyads proved to be nonspecific and inefficient photocatalysts, producing mixtures of CO and H_2, with TNs CO amounting to less than one.[75] Kasuga and co-workers later reported dyads with a Co(III) or Ni(II) Bpy catalytic site,[76] but again CO_2 reduction was not selective. The systems produced mixtures of H_2, CO, and formic acid, and TNs CO were lower than 5.[75] Further, greater yields of photoreduction products were obtained, for the most part, when the sensitizer and catalyst were used as separate entities.

More recent studies of dyads with Ru(Bpy)$_3^{2+}$-like chromophores have extended to heteronuclear complexes with a Re(I)Bpy catalytic component. Ishitani and co-workers were the first to study such systems[21] and have since developed the most effective of these Ru(Bpy)$_3$–Re(I)Bpy dyads, a photocatalyst capable of producing greater than 230 TNs CO.[25,27] Through their studies the authors have initiated a set of principles for constructing effectual two-component photocatalysts, putting emphasis on (1) slow rates of electron transfer from the chromophore to the catalyst—as CO_2 reduction itself is the rate-limiting process; (2) the ancillary ligand bound to the Re(I)Bpy catalyst (i.e., P(OEt)$_3$, pyridine, halide, etc.); (3) directional electron transfer into the bridging diimine ligand of the chromophore; and (4) the use of an aliphatic, nonconjugated connection between chromophore and catalyst. In contrast to the earlier studies of dyads with Ni(II) or Co(III) catalytic sites, the dyads reported by Ishitani tend to outperform systems with the sensitizer and catalyst as separate components. More recently, Bian et al. have demonstrated Ru(Bpy)$_3$–Re(I)Bpy dyads that hold up Ishitani's principles, particularly that an aliphatic link between Ru(Bpy)$_3$ and Re(I)Bpy proves a better photocatalyst than the conjugated analogue.[26]

To the best of our knowledge there is only one other report of a dyad that uses a metalloporphyrin sensitizer covalently linked to a Re(I)Bpy catalytic site for the photoconversion of CO_2 to CO. The preliminary study of a Zn(II) porphyrin–Re(I)Bpy dyad, having a similar molecular structure to that of **[Re(CO)$_3$(Pic)Bpy-PdTPP][PF$_6$]**, appeared to undergo ultrafast electron transfer from the Zn(II) porphyrin to the Re(I)Bpy catalyst upon S_2 excitation, but showed minimal efficiency for CO_2 reduction with a quantum yield of 0.0064 for CO production.[38] Charge recombination was thought to compete with electron transfer quenching from the sacrificial donor and limit catalytic activity. However, in that report the authors did not take into account that the Zn(II) porphyrin precoordinates sacrificial NEt_3, and transfers an electron by an *intra*molecular process.[36,40,77,78] While other Zn(II) porphyrin–Re(I)Bpy dyads have been synthesized by Casanova et al.,[39] the complexes were not tested for photochemical CO_2 reduction. Interestingly, in a separate study Zhang et al. report the photochemical production of H_2 using a dyad with Zn(II) porphyrin and a cobaloxime catalyst in place of Re(I)Bpy.[40] With that dyad the authors obtained TNs H_2 on the order of ~25, and there is no mention of photoreduction at the Zn(II) porphyrin core.

The dyad **[Re(CO)$_3$(Pic)Bpy-PdTPP][PF$_6$]** reported here for the photoreduction of CO_2 to CO results in only 2 TNs CO, detectable after an induction period, and requires excitation into the Soret (S_2) band. The complex undergoes competing reduction reactions at the porphyrin core that form chlorin and bacteriochlorin side products. When sensitizer and catalyst are used as two separate components in place of the dyad, higher TNs CO, up to 9 with PdTPC chromophore, are obtained. This observation is an indication that back-electron transfer from the charge-separated state is a limiting factor for **[Re(CO)$_3$(Pic)Bpy-PdTPP][PF$_6$]** to function as a dyad, though a two-component system still requires collision between compounds.[79]

TRIR Product Assignment. *Picosecond Time Scale.* The TRIR measurements in the region (ca. 1800–2100 cm^{-1}) are sensitive to the oxidation state of Re(I) and the LUMO on the Bpy, as well as mildly sensitive to the peripheral ligand bound to Re(I), 3-picoline for the current case. The TRIR spectrum is much less sensitive to the state of the Pd(II) porphyrin component of the dyad. In the ps-TRIR experiments, both in the presence and absence of NEt_3, a reduced species of **[Re(CO)$_3$(Pic)Bpy-PdTPP][PF$_6$]** can be detected, with product bands shifted to lower wavenumber relative to the ground state complex. This shift is indicative of a reduction at the Re(I)Bpy moiety,[29,80–82] likely to be localized on the lowest unoccupied molecular orbital (LUMO) of the coordinated Bpy, which leads to weakening of the CO bond because of increased back-bonding with Re(I). The excited-state bands appear at the same wavenumber in both picosecond experiments, but have differing kinetic lifetimes. Because it is not possible to distinguish between a charge-separated (CS) state, **[Re$^+$(CO)$_3$(Pic)Bpy$^{\bullet-}$-PdTPP$^{\bullet+}$]**, and a radical species, **[Re$^+$(CO)$_3$(Pic)Bpy$^-$-PdTPP]**, with TRIR spectroscopy, we have distinguished between these product assignments based on the kinetics.

In the ps-TRIR experiments the growth and decay of product bands at 2008 and 1908 cm^{-1} is so rapid that we suggest the reduced species to be a CS state complex, **[Re$^+$(CO)$_3$(Pic)-Bpy$^{\bullet-}$-PdTPP$^{\bullet+}$]**. In other words, upon laser excitation an electron–hole pair is formed in 3–6 ps, the hole being at the PdTPP$^{\bullet+}$ core and the electron at the Re(I)Bpy$^{\bullet-}$ center. The charge recombination then occurs within 30–45 ps. The small changes in lifetimes are probably caused, at least in part, by changes in solvent dynamics. While the band at 2029 cm^{-1} develops on a subpicosecond time scale, its decay time (20–30 ps) is similar to the other, CS excited-state bands, and has been tentatively assigned to a π–π^* transition by comparison to the

dx.doi.org/10.1021/ic200243y | Inorg. Chem. 2011, 50, 11877–11889

results obtained previously in the ps-TRIR experiments for the analogous $[Re(CO)_3(Pic)Bpy\text{-}ZnTPP][PF_6]$ complex.[36]

The apparent inconsistencies in the kinetics of the product bands assigned to $\pi-\pi^*$ and charge-separated excited-states are of particular concern. One plausible explanation is that **$[Re(CO)_3(Pic)Bpy\text{-}PdTPP][PF_6]$** adopts multiple conformations in solution.[36] As a result, the rates of forward and back electron transfer, as determined by ps-TRIR, are dependent on the torsional angles between the planes of the different molecular constituents: PdTPP porphyrin, Re(I)Bpy, and the phenylamide bridge that links them together. The solid state X-ray structure of **$[Re(CO)_3(NCS)Bpy\text{-}PdTPP]$** gives insight into one possible conformation (Figure 2, Table 2). The data show that the phenylamide link is virtually coplanar within itself (178.1(7)°), but is slightly out of plane with the Re(I)Bpy, by nearly 23°, and is substantially distorted from the core plane of the Pd(II) porphyrin having a torsional angle of 69.1(9)°. Conformers that resemble the solid state **$[Re(CO)_3(NCS)\text{-}Bpy\text{-}PdTPP]$** will most likely have a higher population than conformers that are nearly coplanar,[36] but there will still be a distribution of conformers. The ps-TRIR data are therefore a summation of the contributions of different conformers and excited-state conformers present in solution, and may adopt a different distribution in CH_2Cl_2 from that in CH_2Cl_2 with 1 M NEt_3. Alternatively, another kinetic model postulates an ultrafast equilibrium between $\pi-\pi^*$ and CS states.[36] This model gives significance to the only slightly favorable thermodynamic driving force for intramolecular electron transfer from Pd(II) porphyrin S_1 excited-state to Re(I)Bpy, estimated to be $\Delta G_{ox}^* = -0.08$ eV.

Nanosecond Time Scale. While the TRIR spectra in the nanosecond regime are similar in structure to those on the picosecond time scale, the kinetics are clearly different. There is no evidence for a $\pi-\pi^*$ excited-state in the ns-TRIR, but product bands at 2008 and 1903 cm^{-1} grow and decay in about 1 and 10 μs in CH_2Cl_2, respectively, and about 2 and 45 μs in CH_2Cl_2 with 1 M NEt_3, respectively. The product bands observed in the ns-TRIR are tentatively assigned to a charge-separated excited-state complex, *different* from the CS excited-state complex observed in the ps-TRIR experiments. In addition to changes in solvent dynamics in the presence of 1 M NEt_3, two other processes enter the frame on such long time scales: (a) substitution of coordinated picoline by NEt_3, (b) formation of porphyrin reduction products (especially chlorin). It would be difficult to distinguish an excited state complex with coordinated NEt_3 from one with coordinated picoline using TRIR spectroscopy. Porphyrin reduction products should be observable by transient absorption. We tried such experiments on pico and nanosecond time scales (but not microsecond) and observed no evidence for chlorins.

At this stage the assignment of the bands that overlap with the parent bleach in both the ps- and the ns-TRIR experiments is unclear. These bands form at 2035 and 1935 cm^{-1} in the later stages of the ps-TRIR, as the transient bands are recovering. They are present in the very early stages of the ns-TRIR experiments, and decay at the same rate as the bleach of the parent bands.

Differences in Time Scales: from Picoseconds up to Steady-State Conditions. There appears to be some disparity when comparing the kinetics of the product bands of **$[Re(CO)_3(Pic)Bpy\text{-}PdTPP][PF_6]$** in the time-resolved IR experiments, starting from ps-TRIR and working up to steady-state conditions. The ps-TRIR is dominated by ultrafast charge-separation and subsequent recombination, with *full* recovery of ground state complex in a few picoseconds. Nanosecond TRIR experiments give evidence to a *different* CS excited-state species that grows and decays in microseconds, but without full recovery of the ground state complex. In microsecond TRIR experiments that follow a single laser shot of **$[Re(CO)_3(Pic)\text{-}Bpy\text{-}PdTPP][PF_6]$** in the presence of excess bromide, the same CS excited-state complex as that observed in the ns-TRIR can be detected (Supporting Information, Figure S13). When the same system is pulsed for 3 s (at 10 Hz), a *different*, long-lived species is then detected and has been tentatively assigned to a one-electron reduced (OER) species, **$[Re^+(CO)_3(Pic)Bpy^-\text{-}PdTPP]$**. The OER species and the photosubstituted product, **$[Re(CO)_3BrBpy\text{-}PdTPP]$**, decay and grow at the same rate on the order of seconds, but the kinetics are hardly trivial (Supporting Information, Figure S13). It is not possible to make unambiguous assignments for these processes. They are complicated by photosubstitution of Pic by NEt_3, electronic states of the electron-rich asymmetric porphyrin core, different geometric conformers, and porphyrin reduction products that may be in solution.

CONCLUSIONS

We have studied in detail the photophysical and photochemical properties of a molecular dyad made up of a Pd(II) metalloporphyrin sensitizer covalently linked to a cationic Re(I) tricarbonyl bipyridine complex. The pendant arm linking the porphyrin to the Bpy is distinctly twisted in the structure of the NCS derivative. Steady-state photolysis of **$[Re(CO)_3(Pic)\text{-}Bpy\text{-}PdTPP][PF_6]$** with λ_{ex} = 520 nm causes substitution of the labile 3-picoline ligand. When employed as a single component for the photoreduction of CO_2, **$[Re(CO)_3(Pic)\text{-}Bpy\text{-}PdTPP][PF_6]$** produces 2 TNs CO when using λ_{ex} > 420 nm light and only trace amounts of CO when using λ_{ex} = 520 nm light, and the reaction is complicated by photoreduction to chlorin. The two-component system involving PdTPP or PdTPC and $[Re(CO)_3(Pic)Bpy][PF_6]$ is slightly better for CO formation, but still lacks the efficacy of the analogous two-component system with $[Ru(Bpy)_3][PF_6]_2$ as the sensitizer. As an alternative approach, one might envisage increasing the separation between sensitizer and catalyst within a dyad, and we are currently investigating such methodology. The two systems in this study that were found to be most effective for the photoreduction of CO_2,[64] were the mixture of PdTPC: $[Re(CO)_3(Pic)Bpy][PF_6]$ and the mixture of $[Ru(Bpy)_3][PF_6]_2$:$[Re(CO)_3(Pic)Bpy][PF_6]$, giving 9 TNs of CO after 4 h photolysis with λ_{ex} > 420 nm for the former and 11 TNs CO with λ_{ex} > 495 nm for the latter. TRIR spectroscopy of **$[Re(CO)_3(Pic)Bpy\text{-}PdTPP][PF_6]$** with excitation at λ = 532 nm on a picosecond time scale shows formation of a CS state. The ensuing rapid back electron transfer is a significant limitation of this dyad. Investigation by TRIR spectroscopy on longer time scales reveals further species that are kinetically distinct from the CS state, but have similar IR spectra in the ν(CO) region.

ASSOCIATED CONTENT

Supporting Information

Additional ^{1}H NMR, UV−vis, and emission spectra, cif file of **$[Re(CO)_3(NCS)Bpy\text{-}PdTPP]\cdot C_6H_6$**, cyclic voltammograms, kinetics of photosubstitution, Stern−Volmer plot, and a summary of the photoreduction of CO_2 in the presence of

dx.doi.org/10.1021/ic200243y | Inorg. Chem. 2011, 50, 11877–11889

BNAH. This material is available free of charge via the Internet at http://pubs.acs.org.

AUTHOR INFORMATION

Corresponding Author

*E-mail: robin.perutz@york.ac.uk (R.N.P.), mike.george@nottingham.ac.uk (M.W.G.).

ACKNOWLEDGMENTS

The authors wish to thank the EPSRC for funding (projects EP/F047770/1 and EP/F047789/1) and our collaborators in the Consortium for Artificial Photosynthesis (SolarCAP). We thank the EPSRC National Crystallography Service synchrotron component operated by Newcastle University at Diamond Light Source beamline I19 for X-ray data collection for [**Re(CO)$_3$(NCS)Bpy-PdTPP**]. We also acknowledge Dr. Richard E. Douthwaite for use of the radiometer. MWG gratefully acknowledges receipt of a Royal Society Wolfson Merit Award.

REFERENCES

(1) Gray, H. B. *Nature Chem.* **2009**, *1*, 7.
(2) Barber, J. *Chem. Soc. Rev.* **2009**, *38*, 185−196.
(3) Morris, A. J.; Meyer, G. J.; Fujita, E. *Acc. Chem. Res.* **2009**, *42*, 1983−1994.
(4) Roy, S. C.; Varghese, O. K.; Paulose, M.; Grimes, C. A. *ACS Nano* **2010**, *4*, 1259−1278.
(5) Yui, T.; Tamaki, Y.; Sekizawa, K.; Ishitani, O. *Top. Curr. Chem.* **2011**, *303*, 151−184.
(6) Darensbourg, D. J. *Inorg. Chem.* **2010**, *49*, 10765−10780.
(7) Hoffmann, M. R.; Moss, J. A.; Baum, M. M. *Dalton Trans.* **2011**, *40*, 5151−5158.
(8) Hebrard, F.; Kalck, P. *Chem. Rev.* **2009**, *109*, 4272−4282.
(9) Leckel, D. *Energy Fuels* **2009**, *23*, 2342−2358.
(10) Benson, E. E.; Kubiak, C. P.; Sathrum, A. J.; Smieja, J. M. *Chem. Soc. Rev.* **2009**, *38*, 89−99.
(11) Rakowski DuBois, M.; DuBois, D. L. *Acc. Chem. Res.* **2009**, *42*, 1974−1982.
(12) Savéant, J.-M. *Chem. Rev.* **2008**, *108*, 2348−2378.
(13) Hawecker, J.; Lehn, J.-M.; Ziessel, R. *J. Chem. Soc., Chem. Commun.* **1983**, 536−538.
(14) Hawecker, J.; Lehn, J. M.; Ziessel, R. *Helv. Chim. Acta* **1986**, *69*, 1990−2012.
(15) Hawecker, J.; Lehn, J. M.; Ziessel, R. *J. Chem. Soc., Chem. Commun.* **1985**, 56−58.
(16) Lehn, J. M.; Ziessel, R. *Proc. Natl. Acad. Sci. U.S.A.* **1982**, *79*, 701−704.
(17) Agarwal, J.; Johnson, R. P.; Li, G. *J. Phys. Chem. A* **2011**, *115*, 2877−2881.
(18) Takeda, H.; Koike, K.; Inoue, H.; Ishitani, O. *J. Am. Chem. Soc.* **2008**, *130*, 2023−2031.
(19) Hayashi, Y.; Kita, S.; Brunschwig, B. S.; Fujita, E. *J. Am. Chem. Soc.* **2003**, *125*, 11976−11987.
(20) Kirgan, R. A.; Sullivan, B. P.; Rillema, D. P. *Top. Curr. Chem.* **2007**, *281*, 45−100.
(21) Gholamkhass, B.; Mametsuka, H.; Koike, K.; Tanabe, T.; Furue, M.; Ishitani, O. *Inorg. Chem.* **2005**, *44*, 2326−2336.
(22) Bian, Z.-Y.; Sumi, K.; Furue, M.; Sato, S.; Koike, K.; Ishitani, O. *Inorg. Chem.* **2008**, *47*, 10801−10803.
(23) Bian, Z.-Y.; Sumi, K.; Furue, M.; Sato, S.; Koike, K.; Ishitani, O. *Dalton Trans.* **2009**, 983−993.
(24) Koike, K.; Naito, S.; Sato, S.; Tamaki, Y.; Ishitani, O. *J. Photochem. Photobiol., A* **2009**, *207*, 109−114.
(25) Takeda, H.; Ishitani, O. *Coord. Chem. Rev.* **2010**, *254*, 346−354.
(26) Bian, Z.-Y.; Chi, S.-M.; Li, L.; Fu, W. *Dalton Trans.* **2010**, *39*, 7884−7887.
(27) Sato, S.; Koike, K.; Inoue, H.; Ishitani, O. *Photochem. Photobiol. Sci.* **2007**, *6*, 454−461.
(28) Hori, H.; Johnson, F. P. A.; Koike, K.; Ishitani, O.; Ibusuki, T. *J. Photochem. Photobiol., A* **1996**, *96*, 171−174.
(29) Koike, K.; Hori, H.; Ishizuka, M.; Westwell, J. R.; Takeuchi, K.; Ibusuki, T.; Enjouji, K.; Konno, H.; Sakamoto, K.; Ishitani, O. *Organometallics* **1997**, *16*, 5724−5729.
(30) Kurz, P.; Probst, B.; Spingler, B.; Alberto, R. *Eur. J. Inorg. Chem.* **2006**, 2966−2974.
(31) Tsubaki, H.; Sekine, A.; Ohashi, Y.; Koike, K.; Takeda, H.; Ishitani, O. *J. Am. Chem. Soc.* **2005**, *127*, 15544−15555.
(32) Ishitani, O.; George, M. W.; Ibusuki, T.; Johnson, F. P. A.; Koike, K.; Nozaki, K.; Pac, C. J.; Turner, J. J.; Westwell, J. R. *Inorg. Chem.* **1994**, *33*, 4712−4717.
(33) Hori, H.; Ishihara, J.; Koike, K.; Takeuchi, K.; Ibusuki, T.; Ishitani, O. *J. Photochem. Photobiol., A* **1999**, *120*, 119−124.
(34) Aspley, C. J.; Lindsay Smith, J. R.; Perutz, R. N. *J. Chem. Soc., Dalton Trans.* **1999**, 2269−2271.
(35) Gabrielsson, A.; Hartl, F.; Lindsay Smith, J. R.; Perutz, R. N. *Chem. Commun.* **2002**, 950−951.
(36) Gabrielsson, A.; Hartl, F.; Zhang, H.; Lindsay Smith, J. R.; Towrie, M.; Vlcek, A.; Perutz, R. N. *J. Am. Chem. Soc.* **2006**, *128*, 4253−4266.
(37) Gabrielsson, A.; Lindsay Smith, J. R.; Perutz, R. N. *Dalton Trans.* **2008**, 4259−4269.
(38) Kiyosawa, K.; Shiraishi, N.; Shimada, T.; Masui, D.; Tachibana, H.; Takagi, S.; Ishitani, O.; Tryk, D. A.; Inoue, H. *J. Phys. Chem. C* **2009**, *113*, 11667−11673.
(39) Casanova, M.; Zangrando, E.; Iengo, E.; Alessio, E.; Indelli, M. T.; Scandola, F.; Orlandi, M. *Inorg. Chem.* **2008**, *47*, 10407−10418.
(40) Zhang, P.; Wang, M.; Li, C.; Li, X.; Dong, J.; Sun, L. *Chem. Commun.* **2010**, *46*, 8806−8808.
(41) Lees, A. J. *Anal. Chem.* **1996**, *68*, 226−229.
(42) Towrie, M.; Grills, D. C.; Dyer, J.; Weinstein, J. A.; Matousek, P.; Barton, R.; Bailey, P. D.; Subramaniam, N.; Kwok, W. M.; Ma, C.; Phillips, D.; Parker, A. W.; George, M. W. *Appl. Spectrosc.* **2003**, *57*, 367−380.
(43) Brennan, P.; George, M. W.; Jina, O. S.; Long, C.; McKenna, J.; Pryce, M. T.; Sun, X.-Z.; Vuong, K. Q. *Organometallics* **2008**, *27*, 3671−3680.
(44) Rigaku images were converted to Apex II images using the code called "eclipse" written by Professor Simon Parsons of The University of Edinburgh.
(45) *APEX2 software*; Bruker AXS: Madison, WI, 2009.
(46) Sheldrick, G. M. *SHELXS-97, a program for crystal structure solution*; Göttingen University: Göttingen, Germany, 1997.
(47) Sheldrick, G. M. *SHELXL-97, a program for crystal structure determination*; Göttingen University: Göttingen, Germany, 1997.
(48) McGee, K. A.; Veltkamp, D. J.; Marquardt, B. J.; Mann, K. R. *J. Am. Chem. Soc.* **2007**, *129*, 15092−15093.
(49) Kutal, C.; Weber, M. A.; Ferraudi, G.; Geiger, D. *Organometallics* **1985**, *4*, 2161−2166.
(50) Harel, Y.; Manassen, J. *J. Am. Chem. Soc.* **1978**, *100*, 6228−6234.
(51) Whitlock, H. W.; Hanauer, R.; Oester, M. Y.; Bower, B. K. *J. Am. Chem. Soc.* **1969**, *91*, 7485−7489.
(52) Mauzerall, D.; Westheimer, F. H. *J. Am. Chem. Soc.* **1955**, *77*, 2261−2264.
(53) Schanze, K. S.; Lee, L. Y. C.; Giannotti, C.; Whitten, D. G. *J. Am. Chem. Soc.* **1986**, *108*, 2646−2655.
(54) Ion, R. M.; Mandravel, C.; Bercu, C. *Rev. Chim.* **1998**, *49*, 121−127.
(55) Sapunov, V. V.; Egorova, G. D. *Russ. J. Phys. Chem. A* **1992**, *66*, 471−477.
(56) Sapunov, V. V.; Egorova, G. D. *J. Appl. Spectrosc.* **1989**, *50*, 611−615.
(57) Sapunov, V. V.; Egorova, G. D. *J. Appl. Spectrosc.* **1987**, *46*, 519−522.
(58) Sapunov, V. V.; Solov'ev, K. N. *Vestsi Akad. Navuk BSSR, Ser. Fiz.-Mat. Navuk* **1980**, 60−64.

(59) Sapunov, V. V.; Solov'ev, K. N.; Egorova, G. D. *Russ. J. Phys. Chem. B* **1986**, *5*, 1044−1048.
(60) Blanco Rodriguez, A. M.; Gabrielsson, A.; Motevalli, M.; Matousek, P.; Towrie, M.; Sebera, J.; Zalis, S.; Vlček, A. *J. Phys. Chem. A* **2005**, *109*, 5016−5025.
(61) Fleischer, E. B.; Miller, C. K.; Webb, L. E. *J. Am. Chem. Soc.* **1964**, *86*, 2342−2347.
(62) The absolute quantum yield (φ) for product formation was determined to be $\varphi = 0.12 \pm 0.01$. Although the efficiency for this photoreaction was calculated using a procedure that accounts for substantial inner filter effects[41] between the reactant and the product, there was some evidence for an induction period that makes the quantum yield difficult to interpret. In each experiment we observed transformation of [**Re(CO)$_3$(Pic)Bpy-PdTPP**][**PF$_6$**] to [**Re(CO)$_3$BrBpy-PdTPP**]; reproducibility was complicated by a variation of both the induction period and the rate of the photoreaction. The efficiency reported is for the experiment with a minimal induction period.
(63) Mercer-Smith, J. A.; Sutcliffe, C. R.; Schmehl, R. H.; Whitten, D. G. *J. Am. Chem. Soc.* **1979**, *101*, 3995−3997.
(64) When 0.1 M BNAH is added to the reaction mixture, more TNs CO are formed. However, the reaction becomes quite complicated, and we do not understand the effect of the BNAH at this point. Details of preliminary experiments are outlined in the Supporting Information.
(65) Giraudeau, A.; Callot, H. J.; Gross, M. *Inorg. Chem.* **1979**, *18*, 201−206.
(66) Sacksteder, L.; Zipp, A. P.; Brown, E. A.; Streich, J.; Demas, J. N. *Inorg. Chem.* **1990**, *29*, 4335−4340.
(67) Turro, N. J. *Modern Molecular Photochemistry*, 2nd ed.; The Benjamin/Cummings Publishing Company, Inc.: Menlo Park, 1978; p 628.
(68) Easun, T. L.; Alsindi, W. Z.; Towrie, M.; Ronayne, K. L.; Sun, X.-Z.; Ward, M. D.; George, M. W. *Inorg. Chem.* **2008**, *47*, 5071−5078.
(69) Butler, J. M.; George, M. W.; Schoonover, J. R.; Dattelbaum, D. M.; Meyer, T. J. *Coord. Chem. Rev.* **2007**, *251*, 492−514.
(70) Vergeer, F. W.; Kleverlaan, C. J.; Matousek, P.; Towrie, M.; Stufkens, D. J.; Hartl, F. *Inorg. Chem.* **2005**, *44*, 1319−1331.
(71) Picosecond transient UV/visible data showed that excitation (λ_{ex} = 532 nm) in CH_2Cl_2 leads to production of an intense band at 450 nm within the rise time of the instrument (<1 ps). This decays partially over the first 10−30 ps and then fully within a few hundred picoseconds, i.e., on a similar time scale as the rise of the band at 2035 and 1935 cm^{-1} in the ps-TRIR.
(72) Kimura, E.; Bu, X.; Shionoya, M.; Wada, S.; Maruyama, S. *Inorg. Chem.* **1992**, *31*, 4542−4546.
(73) Kimura, E.; Wada, S.; Shionoya, M.; Okazaki, Y. *Inorg. Chem.* **1994**, *33*, 770−778.
(74) Beley, M.; Collin, J. P.; Ruppert, R.; Sauvage, J. P. *J. Am. Chem. Soc.* **1986**, *108*, 7461−7467.
(75) While TNs CO were not reported by the authors, they can be inferred from their data.
(76) Komatsuzaki, N.; Himeda, Y.; Hirose, T.; Sugihara, H.; Kasuga, K. *Bull. Chem. Soc. Jpn.* **1999**, *72*, 725−731.
(77) Kluwer, A. M.; Kapre, R.; Hartl, F.; Lutz, M.; Spek, A. L.; Brouwer, A. M.; van Leeuwen, P. W. N. M.; Reek, J. N. H. *Proc. Natl. Acad. Sci. U.S.A.* **2009**, *106*, 10460−10465.
(78) Li, X.; Wang, M.; Zhang, S.; Pan, J.; Na, Y.; Liu, J.; Akermark, B.; Sun, L. *J. Phys. Chem. B* **2008**, *112*, 8198−8202.
(79) If we use the Stern−Volmer constant of K_{SV} = 24 M^{-1} quenching of PdTPP by NEt_3 in CH_2Cl_2 solution (Supporting Information, Figure S10) and a literature value for the excited-state lifetime of PdTPP, τ_0 = 385 μs (Harriman, A. *J. Chem. Soc., Faraday 1200 Trans. 2* **1981**, *77*, 1281−1291) in the absence of quencher, we obtain a quenching constant, $k_q = 6.5 \times 10^4$ M^{-1} s^{-1}. It is therefore expected that emission quenching of PdTPP or [**Re(CO)$_3$(Pic)Bpy-PdTPP**][**PF$_6$**] by NEt_3 will occur under photochemical CO_2 reduction conditions, i.e., 5:1 (v/v) DMF:NEt_3 (1.2 M NEt_3) with a pseudo first order rate constant of ca. 10^4 to 10^5 s^{-1}.
(80) Johnson, F. P. A.; George, M. W.; Hartl, F.; Turner, J. J. *Organometallics* **1996**, *15*, 3374−3387.
(81) Stor, G. J.; Hartl, F.; van Outersterp, J. W. M.; Stufkens, D. J. *Organometallics* **1995**, *14*, 1115−1131.
(82) van Outersterp, J. W. M.; Hartl, F.; Stufkens, D. J. *Organometallics* **1995**, *14*, 3303−3310.

NOTE ADDED AFTER ASAP PUBLICATION

This article was published on the Web on November 1, 2011. Due to a production error, text changes were not incorporated in this version. The corrected version was reposted on November 2, 2011.